Journal of Engineering Science and Technology
Vol. 8, No. 1 (2013) 1 - 15

NUMERICAL INVESTIGATION FOR THE HEAT TRANSFER ENHANCEMENT IN HELICAL CONE COILS OVER ORDINARY HELICAL COILS

M. M. ABO ELAZM[1], A. M. RAGHEB[1,*], A. F. ELSAFTY[2], M. A. TEAMAH[3]

[1]Arab Academy for Science, Technology and Maritime Transport, Alexandria, Egypt
[2]Faculty of Engineering, American University of the Middle East, Kuwait, Kuwait
[3]Faculty of Engineering, Alexandria University, Alexandria, Egypt.
*Corresponding Author: ragheb_9@yahoo.com

Abstract

This numerical research is introducing the concept of helical cone coils and their enhanced heat transfer characteristics compared to the ordinary helical coils. Helical and spiral coils are known to have better heat and mass transfer than straight tubes, which is attributed to the generation of a vortex at the helical coil known as Dean Vortex. The Dean number which is a dimensionless number used to describe the Dean vortex is a function of Reynolds number and the square root of the curvature ratio, so varying the curvature ratio for the same coil would vary the Dean number. Two scenarios were adopted to study the effect of changing the taper angle (curvature ratio) on the heat transfer characteristics of the coil; the commercial software FLUENT was used in the investigation. It was found that Nusselt number increased with increasing the taper angle. A MATLAB code was built based on empirical correlation of Manlapaz and Churchill for ordinary helical coils to calculate the Nusselt number at each coil turn, and then calculate the average Nusselt number for the entire coil turns, the CFD simulation results were found acceptable when compared with the MATLAB results.

Keywords: Numerical, Helical coils, Heat exchanger, Heat transfer.

1. Introduction

Helical coils have been long and widely used as heat exchangers in power, petrochemical, HVAC, chemical and many other industrial processes. Helical and spiral coils are known to have better heat and mass transfer compared to straight tubes, the reason for that is the formation of a secondary flow superimposed on

Nomenclatures

a	Pipe radius, mm
De	Dean number
H	Helical coil height, mm
h	Heat transfer coefficient, W/m^2 K
I	Inclined height, mm
M_{urf}	Relaxation factor of momentum
Nu	Nusselt number.
P	Helical Pitch, mm
P_{urf}	Relaxation factor of pressure
R	Coil radius of curvature, mm
Re	Reynolds number.
Re_{cr}	Critical Reynolds number.
T	Temperature, K
T_{wall}	Wall temperature, K
t	Coil thickness, mm
u	Inlet velocity, m/s
Greek Symbols	
θ	Taper angle, Deg.
ρ	Density, kg/m^3

the primary flow, known as Dean Vortex [1-3]. The Dean Vortex was first observed by Eustice [4]; then numerous studies have been reported on the flow fields that arise in curved pipes [2, 3, 5-10]. The first attempt to mathematically describe the flow in a coiled tube was made by Dean, he found that the secondary flow induced in curved pipes (Dean Vortex) is a function of Reynolds Number and the curvature ratio, the Dean Number is widely used to characterize the flow in curved tubes:

$$\mathrm{De} = \mathrm{Re}\sqrt{\frac{a}{R}} \tag{1}$$

It has been widely observed that the flow inside coiled tubes remains in the viscous regime up to a much higher Reynolds Number than that for straight tubes. The curvature-induced helical vortices (Dean Vortex) tend to suppress the onset of turbulence and delay transition. The critical Reynolds Number which describes the transition from laminar to turbulent flow is given by any correlations; the following correlation is given by Srinivasan et al. [11]:

$$\mathrm{Re}_{cr} = 2100\left(1 + 12\sqrt{\frac{a}{R}}\right) \tag{2}$$

Dennis and Ng [12] numerically studied laminar flow through a curved tube using a finite difference method with emphasis on two versus four vortex flow conditions. They ran simulations in the Dean range of 96 to 5000. The four vortex solutions would only appear for a Dean number greater than 956. Dennis and Riley [13] developed an analytical solution for the fully developed laminar flow for high Dean Numbers. Though they could not find a complete solution to the problem, they stated that there is strong evidence that at high Dean Numbers the flow developed into an inviscid core with a viscous boundary layer at the pipe wall.

The effect of pitch on heat transfer and pressure drop was studied by Austin and Soliman [14] for the case of uniform wall heat flux. The results showed significant pitch effects on both the friction factor and the Nusselt Number at low Reynolds Numbers, though these effects weakened as the Reynolds number increased. The authors suggested that these pitch effects were due to free convection, and thus decrease as the forced convection became more dominant at higher Reynolds Numbers. The effect of the pitch on the Nusselt Number in the laminar flow of helicoidal pipes was also investigated by Yang et al. [15]. Numerical results for fully developed flow with a finite pitch showed that the temperature gradient on one side of the pipe increased with increasing torsion; however, the temperature gradient on the opposite decreased. Overall, the Nusselt Number slightly decreased with increasing torsion for low Prandtl Numbers, but significantly decreased with larger Prandtl Numbers. On the other hand Germano [16] introduced an orthogonal coordinate system to study the effect of torsion and curvature on the flow in a helical pipe. The results of the perturbation method indicated that the torsion had a second order effect and curvature had a first order effect on the flow. Further studies by Tuttle [17] indicated that the frame of reference (coordinate system) determined whether the torsion effect is of the first or second order.

Kalb and Seader [18] numerically studied the heat transfer in helical coils in case of uniform heat flux using an orthogonal toroidal coordinate system. They have found that for Prandtl Numbers greater than 0.7, it was shown that the local Nusselt Number in the area of the inner wall was always less than that of a straight tube, and increasing less as the Dean Number was increased till it reached a limiting value. The local Nusselt Numbers on the outer wall continued to increase with increasing Dean Number. Fully developed laminar flow and heat transfer was studied numerically by Zapryanov et al. [19] using a method of fractional steps for a wide range of Dean (10 to 7000) and Prandtl (0.005 to 2000) numbers. Their work focused on the case of constant wall temperature and showed that the Nusselt number increased with increasing Prandtl numbers, even for cases at the same Dean number.

Spiral coils had received little attention compared to helical coils, though the reported results of spiral coils showed better performance than helical ones [20]. Figueiredo and Raimundo [21] experimentally investigated the thermal response of a hot-water store and the thermal discharge characteristics from heat exchanger coils placed inside. The classical cylindrical coil and the flat spiral coil were investigated. The results indicated that the efficiency of flat spiral coil was higher than that of a cylindrical one. The results from comparison between the model and experiments were in good agreement. Naphon and Suwagrai [22] studied the Effect of curvature ratios on the heat transfer in the horizontal spirally coiled tubes both experimentally and numerically. They have found that due to the centrifugal force, the Nusselt number and pressure drop obtained from the spirally coiled tube are 1.49, 1.50 times higher than those from the straight tube, respectively.

Helical cone coils had even received lower attention than spiral coils, only very few researchers have investigated the capabilities of these coils due to the complexity of the structure, it was hard to investigate it both numerically and experimentally. Yan Ke et al. [23] have investigated the helical cone tube bundles both numerically and still some foregoing experiments, the authors found that the cone angle has a significant effect on enhancing the heat transfer coefficient, also they've found that the pitch has nearly no effect on the heat transfer.

The aim of this paper is to further numerically investigate the effect of the taper angle on Nusselt Number and the heat transfer coefficient for helical cone coils. Finally trying to know the optimum helical cone coil design; through comparing the results of the following two scenarios.

2. Numerical Simulation

2.1. Helical Cone Coil Geometry

The Geometry of the helical cone tube is shown in Fig. 1; both the curvature and torsion are variable along the tube. The bottom radius of curvature is donated R, the pipe diameter a, the helical pitch P, the straight height H and the inclined height I. For a straight helical coil the height, H, will be equal to I but when changing the inclination angle, θ, the height of the coil, I, will change in accordance to that angle, while keeping H constant.

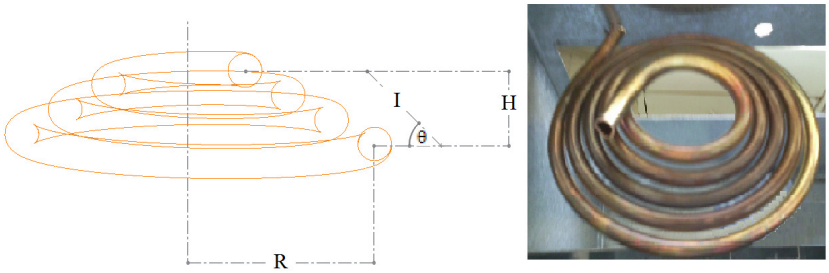

Fig. 1. Helical Coil Geometry.

Three bottom radii of curvatures, R, were used 50, 75 and 100 mm, also two pipe diameters, a, were used; 10 and 12.5 mm. So as to keep the height of the coil, H, constant, the height, I, which changes with respect to the taper angle, θ, was proposed. It should be noted that the helical spiral coil is mainly optimized to be used as a condenser (dehumidifier) for a solar humidification dehumidification desalination unit.

2.2. Simulation Model

The laminar flow in the helical spiral coil is simulated using the commercial CFD software Fluent. In the simulation of the laminar fluid flow, the flow and pressure equations were solved with SIMPLEC algorithm, which is one of the three widely, used velocity pressure coupling algorithm in Fluent. The Second Order Upwind algorithm was employed in the discretization of the equations because of its accuracy and iterating efficiency. The parameters of laminar fluid flow model were in accordance with the default values of the CFD software; $P_{urf} = 0.3$ and $M_{urf} = 0.7$, where, the P_{urf} and M_{urf} respectively denote the Under Relaxation Factor of pressure and momentum of the fluid flow inside the tube during the iterating of the calculation. The commercial software Fluent uses both Navier–Stockes equations, continuity equation and the energy equation in the solution, the equations are solved for laminar, steady and 3D flow.

Navier – Stockes (momentum) equations:

$$\rho\left(\frac{\partial u_r}{\partial t}+u_r\frac{\partial u_r}{\partial r}+\frac{u_\theta}{r}\frac{\partial u_r}{\partial \theta}+u_z\frac{\partial u_r}{\partial z}-\frac{u_\theta^2}{r}\right)=-\frac{\partial p}{\partial r}+\mu\left(\frac{1}{r}\frac{\partial}{\partial r}\left(r\frac{\partial u_r}{\partial r}\right)+\frac{1}{r^2}\frac{\partial^2 u_r}{\partial \theta^2}+\frac{\partial^2 u_r}{\partial z^2}-\frac{u_r}{r^2}-\frac{2}{r^2}\frac{\partial u_\theta}{\partial \theta}\right)+\rho g_r$$

$$\rho\left(\frac{\partial u_\theta}{\partial t}+u_r\frac{\partial u_r}{\partial r}+\frac{u_\theta}{r}\frac{\partial u_\theta}{\partial \theta}+u_z\frac{\partial u_\theta}{\partial z}-\frac{u_r u_\theta}{r}\right)=-\frac{1}{r}\frac{\partial p}{\partial \theta}+\mu\left(\frac{1}{r}\frac{\partial}{\partial r}\left(r\frac{\partial u_\theta}{\partial r}\right)+\frac{1}{r^2}\frac{\partial^2 u_\theta}{\partial \theta^2}+\frac{\partial^2 u_\theta}{\partial z^2}-\frac{u_\theta}{r^2}-\frac{2}{r^2}\frac{\partial u_\theta}{\partial \theta}\right)+\rho g_\theta$$

$$\rho\left(\frac{\partial u_z}{\partial t}+u_r\frac{\partial u_z}{\partial r}+\frac{u_\theta}{r}\frac{\partial u_z}{\partial \theta}+u_z\frac{\partial u_z}{\partial z}\right)=-\frac{\partial p}{\partial z}+\mu\left(\frac{1}{r}\frac{\partial}{\partial r}\left(r\frac{\partial u_z}{\partial r}\right)+\frac{1}{r^2}\frac{\partial^2 u_z}{\partial \theta^2}+\frac{\partial^2 u_z}{\partial z^2}\right)+\rho g_z$$

The continuity equation:

$$\frac{\partial \rho}{\partial t}+\frac{1}{r}\frac{\partial}{\partial r}(\rho r u_r)+\frac{1}{r}\frac{\partial(\rho u_\theta)}{\partial \theta}+\frac{\partial(\rho u_z)}{\partial z}=0$$

2.3. Model Verification

In order to verify the accuracy of the mathematical model being investigating, a preliminary mathematical model for a helical cone coil was built and its results were compared to the experimental results of that coil [9]. Table 1 shows the coil data for the verification numerical/experimental model. During the experiment vapor is admitted to the coil at various vapor temperatures these temperatures were used in the numerical model to see the difference in the results of the numerical model to the experimental results. Figure 2 shows the results of both the numerical and experimental testing. It can be clearly seen that the difference in the coil exit temperature obtained from both the numerical and experimental results is less than 10%.

Table 1. Verification Helical Cone Coil Data.

P (mm)	*R* (mm)	*a* (mm)	Re	*u* (m/s)	*t* (mm)	*H* (mm)	*I* (mm)
20	95	11	6360	0.58	0.6	50	95

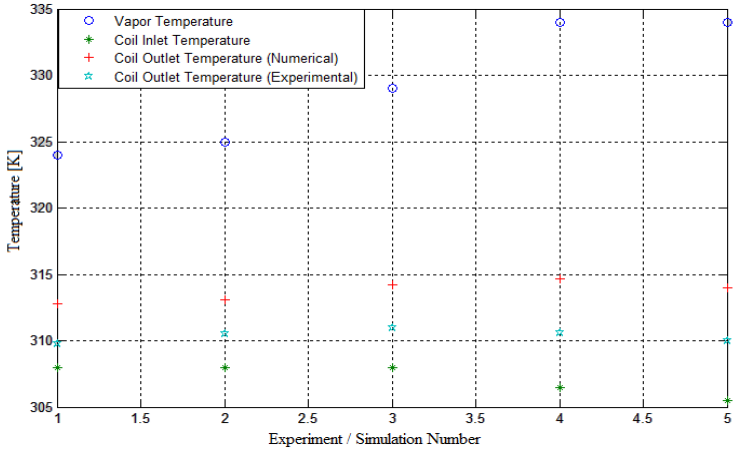

Fig. 2. Comparison of Mathematical and Experimental Results.

3. Results and Discussion

Two scenarios were adopted to study the enhancements in the heat transfer (for the flow inside the coil) made by helical cone coils over the ordinary helical coils; in each scenario twenty two models were built. Table 2 show the difference between the two scenarios.

Table 2. Two Scenarios Data.

Scenario	Pitch	Height
Ordinary Helical Coil	P	H
First Scenario	$P \cos(\theta)$	H
Second Scenario	$P \cos(\theta)$	$H \cos(\theta)$

3.1. First scenario: Taper angle effect

Twenty two models were used to study the effect of the taper angle on the heat transfer coefficient and Nusselt number, where for all cases the values of the wall temperature, T_{wall}, and the inlet velocity, u, are set to 360 K and 0.1 m/s respectively. Table 3 shows the details of these models. To have a better understanding for the results, each bottom radius of curvature, R, and pipe diameter, a, will be discussed separately, then a comparison between them will be made to have a complete understanding for the effect of the taper angle on each case, also to know how to optimize each case.

Table 3. Helical Coil Details.

R (mm)	a (mm)	Re	Θ (Deg.)	I (mm)
70	8	1595	0, 20, 40	25, 26.6, 32.64
	12	2392	0, 25, 40	25, 27.58, 32.64
80	8	1595	0, 20, 50, 60	25, 26.6, 38.9, 50
	12	2392	0, 20, 50, 70	25, 26.6, 38.9, 73.1
90	8	1595	0, 25, 45, 60	25, 27.58, 35.4, 50
	12	2392	0, 20, 40, 70	25, 26.6, 32.64, 73.1

For R = 70, 80, 90 mm and a = 8 mm, Figs. 3(a), 4(a) and 5(a) show the increase in the outlet temperature of the coil with increasing the taper angle (θ). Figures 3(b), 4(b) and 5(b) show that Nusselt number increases with increasing the taper angle too. Finally, Figs. 3(c), 4(c) and 5(c) show the increase in the heat transfer coefficient when increasing the taper angle. It is worth noting that the heat transfer coefficient, Nusselt number and coil outlet temperature increased with increasing the taper angle while utilizing lower space (similar diameter and height as the ordinary helical coil, but the taper angle decrease overall space) which has a significant positive effect on the space utilization in the industrial applications. It should be noted that the increase in the Nusselt number and heat transfer coefficient is logic, as the Nusselt number varies directly with the Dean Number (De) which varies directly with the curvature ratio, a/R. So, as R decreased when increasing the taper angle, the curvature ratio increased; while the increase in the exit temperature is attributed to the

increase in both the area of the coil and the heat transfer coefficient which is a result of increasing the taper angle.

Finally, Figs. 6(a), (b) and (c) represent the angles (0, 20, 40) respectively for R = 70. These figures show the change in the velocity due to the change in the taper angle, and as it can be seen that the velocity increases which means that Reynolds Number is increasing and thus the Dean Number. Also, it could be noted that the center of the main flow is shifted towards the outwards of the pipe (Dean Vortex).

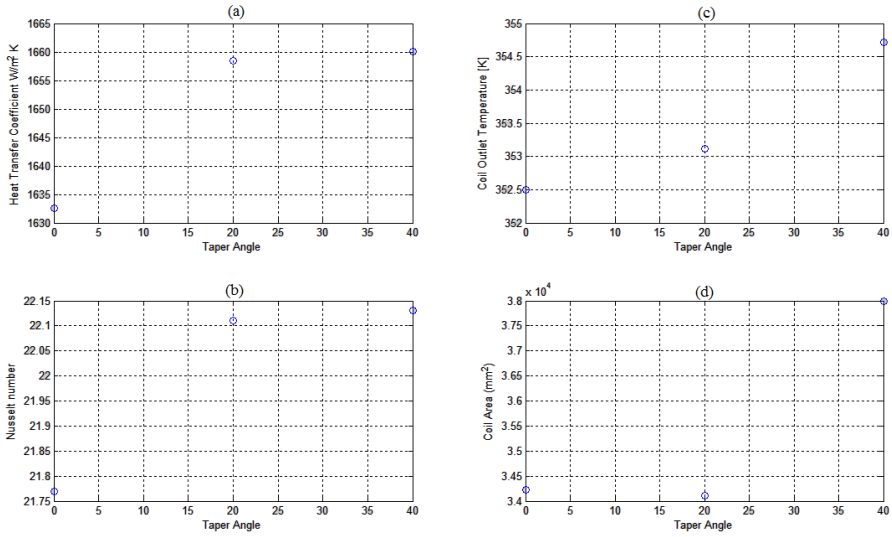

Fig. 3. Effect of the Taper Angle on the Temperature, Heat transfer coefficient and Nusselt number when R = 70.

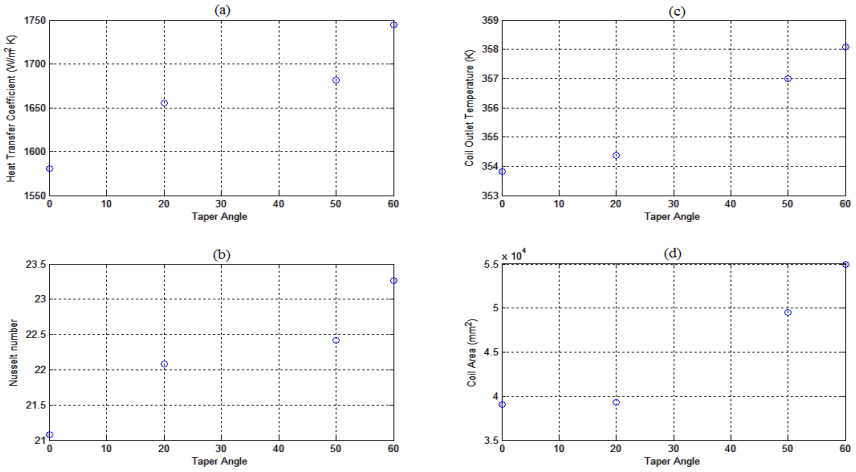

Fig. 4. The Effect of the Taper Angle on the Temperature, Heat Transfer Coefficient and Nusselt Number (R = 80).

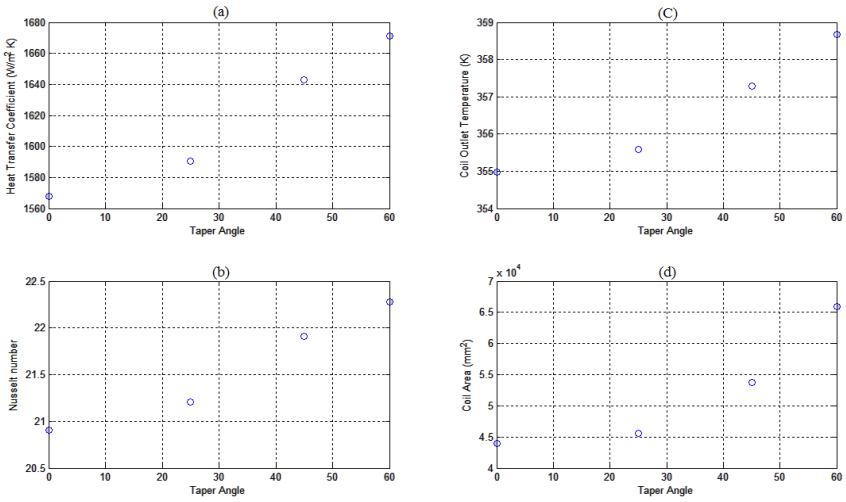

Fig. 5. The Effect of the Taper Angle on the Temperature, Heat Transfer Coefficient and Nusselt Number (R = 90).

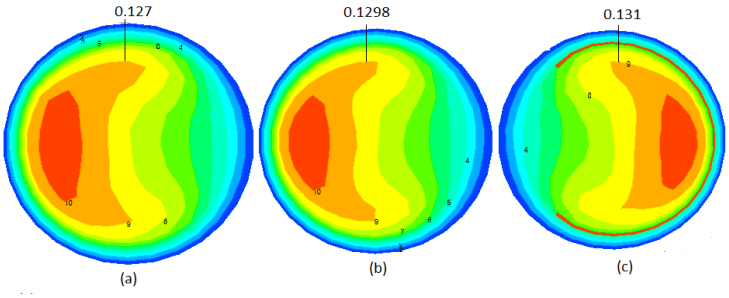

Fig. 6. The Effect of the Taper Angle on the Velocity Profile.

For R = 70, 80, 90 mm and a = 12 mm, Figs. 7(a), 8(a) and 9(a) show the increase in the outlet temperature of the coil with increasing the taper angle (θ). Figures 7(b), 8(b) and 9(b) show that Nusselt Number increases with increasing the taper angle too. Finally, Figs. 7(c), 8(c) and 9(c) show the increase in the heat transfer coefficient when increasing the taper angle. Figures 10(a), (b), and (c) represents the angles (0, 25, 40) respectively for R = 70, these figures show that the centre of the main flow is shifted towards the outwards of the pipe (Dean Vortex). Again the increase in the Nusselt number and heat transfer coefficient is logic, as the Nusselt number varies directly with the Dean number which varies directly with the curvature ratio, a/R. So, as R decreased when increasing the taper angle, the curvature ratio increased; while the increase in the exit temperature is attributed to the increase in both the area of the coil and the heat transfer coefficient which is a result of increasing the taper angle.

It can be clearly seen from the following curves that both the heat transfer coefficient and Nusselt number increases when increasing the taper angle for any bottom radius of curvature, R, and any pipe diameter, a.

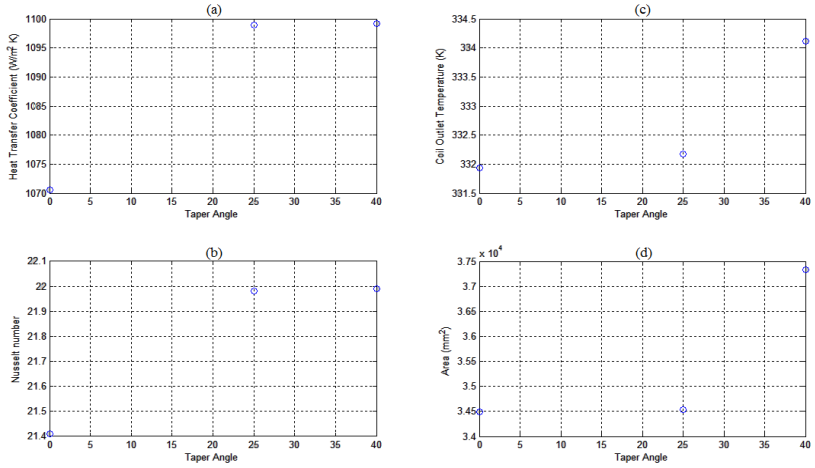

Fig. 7. The Effect of the Taper Angle on the Temperature, Heat Transfer Coefficient and Nusselt Number (R = 70).

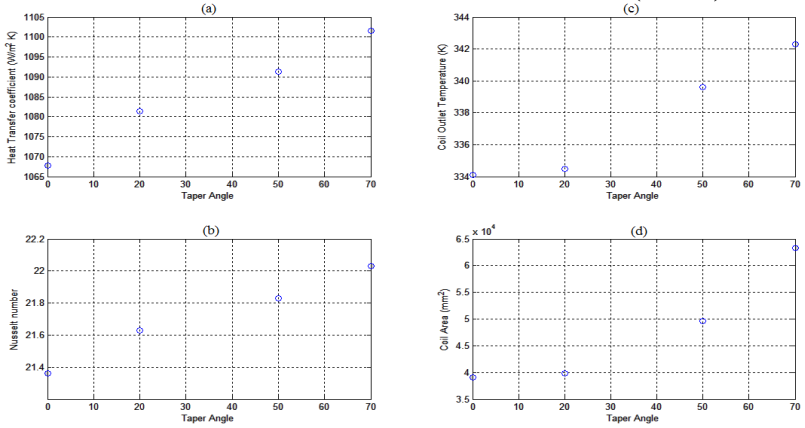

Fig. 8. The Effect of the Taper Angle on the Temperature, Heat Transfer Coefficient and Nusselt Number (R = 80).

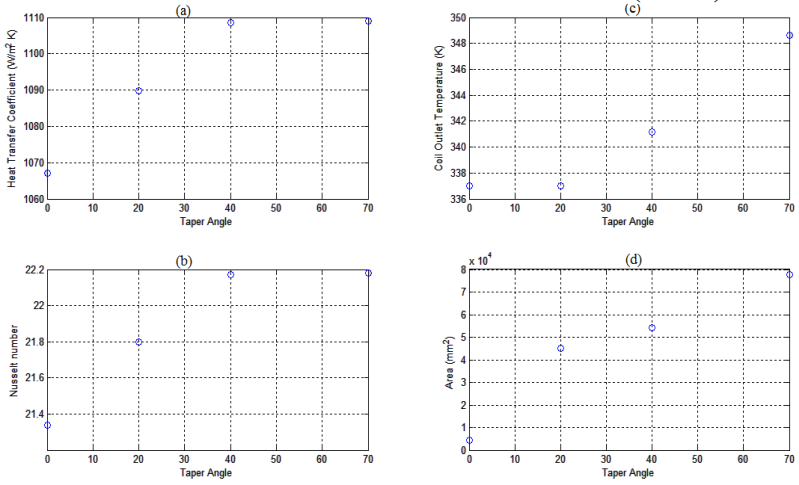

Fig. 9. The Effect of the Taper Angle on the Temperature, Heat Transfer Coefficient and Nusselt Number (R = 90).

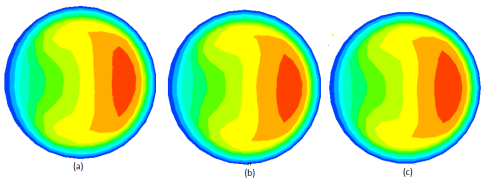

Fig. 10. The Effect of the Taper Angle on the Velocity Profile.

Result Comparison with the MATLAB Code

A comparison between the MATLAB code, which was built based on the experimental equation of Manlapaz and Churchill [24] for ordinary helical coils subjected to constant wall temperature and the CFD results will be discussed in this section, the reason for this comparison is to see whether these equations could be used for the helical cone coils or not. To apply the equations on the helical cone coil, the equation will be calculated for every coil turn then an average value for the Nusselt Number will be evaluated. The comparison will be on one of the previous results only, the model will be with R = 70 and a = 8. From Fig. 11 it could be seen that the equation could be used till taper angle equals to forty but after that error increases significantly and that was attributed to the accumulation of error in the calculations for each turn. The Manlapaz and Churchill equation that resulted from their experimental work is as follow:

$$\mathrm{Nu} = \left[\left(3.657 + \frac{4.343}{x_1}\right)^3 + 1.158\left(\frac{\mathrm{De}}{x_2}\right)^{3/2}\right]^{1/3} \tag{3}$$

where

$$x_1 = \left(1 + \frac{957}{\mathrm{De}^2\, Pr}\right)^2 \tag{4}$$

$$x_2 = 1 + \frac{0.477}{Pr} \tag{5}$$

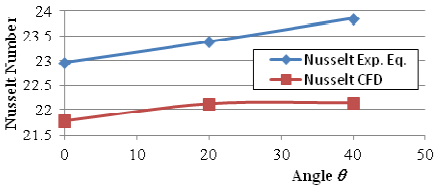

Fig. 11. Nusselt Number from the Experimental Equation vs. Nusselt Number from the CFD Simulation.

3.2. Second scenario: Taper angle effect

Twenty two models were used to study the effect of the taper angle on the heat transfer coefficient and Nusselt Number. Table 4 shows the details of these models, where for all these models the inlet velocity, u, is set to 0.1 m/s. To have a better understanding for the results, each bottom radius of curvature, R, and pipe diameter, a, will be discussed separately, then a comparison between them will be made to have a complete understanding for the effect of the taper angle on each case, also to know how to optimize each case.

Table 4. Helical Coil Details.

R (mm)	*a* (mm)	Re	θ	*H*
50	10	997	0, 20, 40	25, 23.49, 19.15
	12.5	1246		30, 28.19, 22.98
75	10	997	0, 20, 40, 60	33, 31, 25.28, 16.5
	12.5	1246		30, 28.19, 22.98, 15
100	10	997	0, 20, 45, 60	33, 31, 23.33, 16.5
	12.5	1246	0, 20, 40, 60	30, 28.19, 22.48, 15

For R = 50, 75, 100 mm and a = 10 mm, it can be clearly seen from Figs. 12(a), 13(a) and 14(a), that the heat transfer coefficient has increased with increasing the taper angle, θ. Figures 12(c), 13(c) and 14(c) show that Nusselt Number increases with increasing the taper angle too, while Figs. 12(b), 13(b) and 14(b) show that the surface area of heat transfer decreases with increasing the taper angle which leads to a decrease in the exit temperature unlike the first scenario, leading to a decrease in the space required for installation and material used in manufacturing.

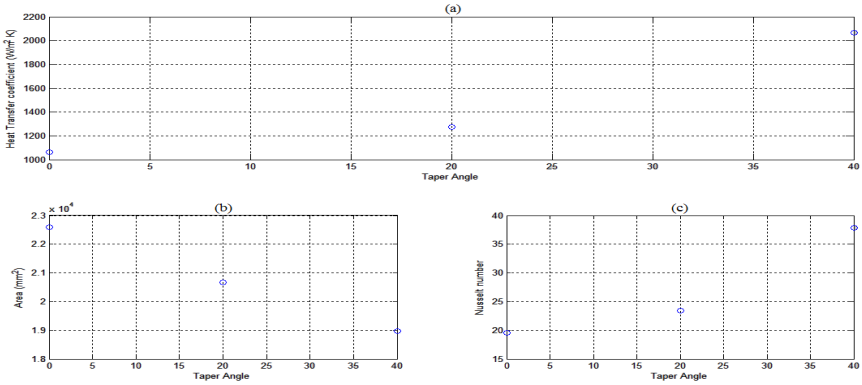

Fig. 12. The Effect of the Taper Angle on the Area, Heat Transfer Coefficient and Nusselt Number (R = 50, a = 10).

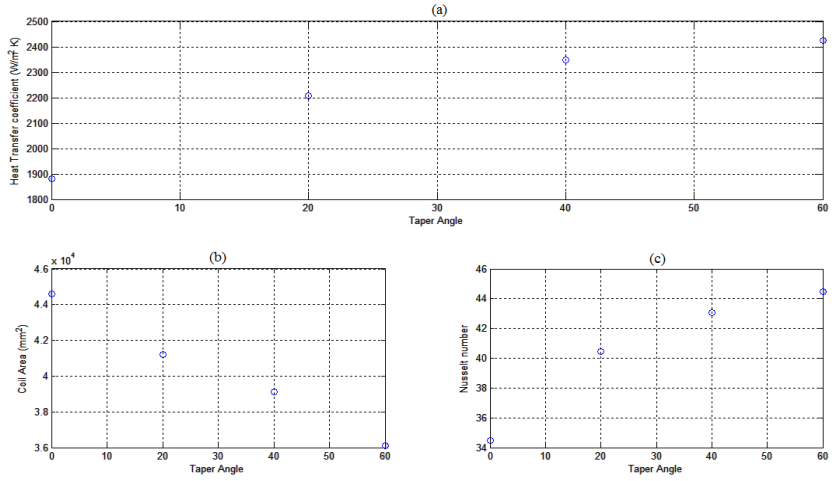

Fig. 13. The Effect of the Taper Angle on the Area, Heat Transfer Coefficient and Nusselt Number (R = 75, a = 10).

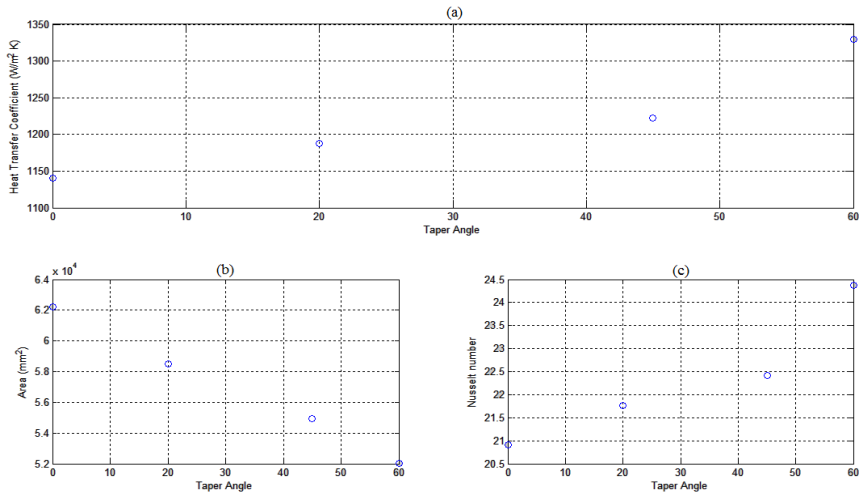

Fig. 14. The Effect of the Taper Angle on the Area, Heat Transfer Coefficient and Nusselt Number (R = 100, a = 10).

For R = 50, 75, 100 mm and a = 12.5 mm, it can also be clearly seen from Figs. 15(a), 16(a) and 17(a) that the heat transfer coefficient increases with increasing the taper angle, while Figs. 15(c), 16(c) and 17(c) show that the Nusselt number increases with increasing the taper angle. It can be clearly seen from the previous curves that both the heat transfer coefficient and Nusselt Number increases when increasing the taper angle for any bottom radius of curvature, R, and any pipe diameter, a. Again the increase in the Nusselt number and heat transfer coefficient is logic, as the Nusselt number varies directly with the Dean number which varies directly with the curvature ratio, a/R. So, as R decreases when increasing the taper angle, the curvature ration increases.

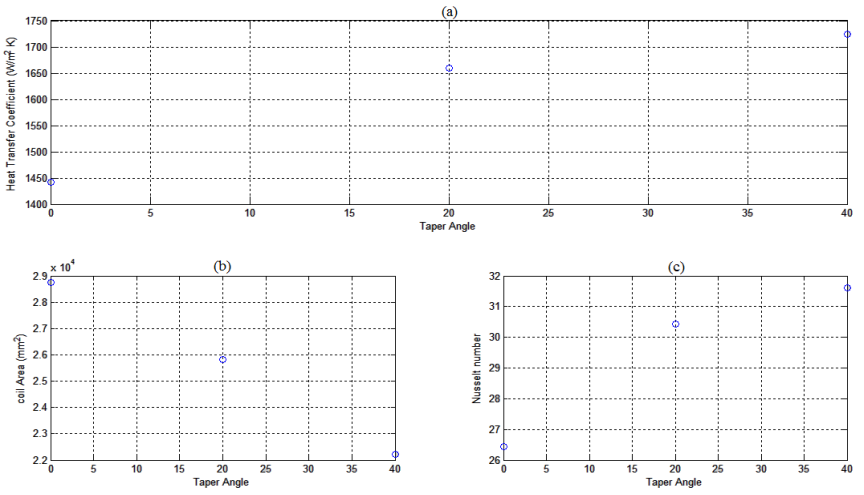

Fig. 15. The Effect of the taper angle on the area, Heat Transfer Coefficient and Nusselt number (R = 50, a = 12.5).

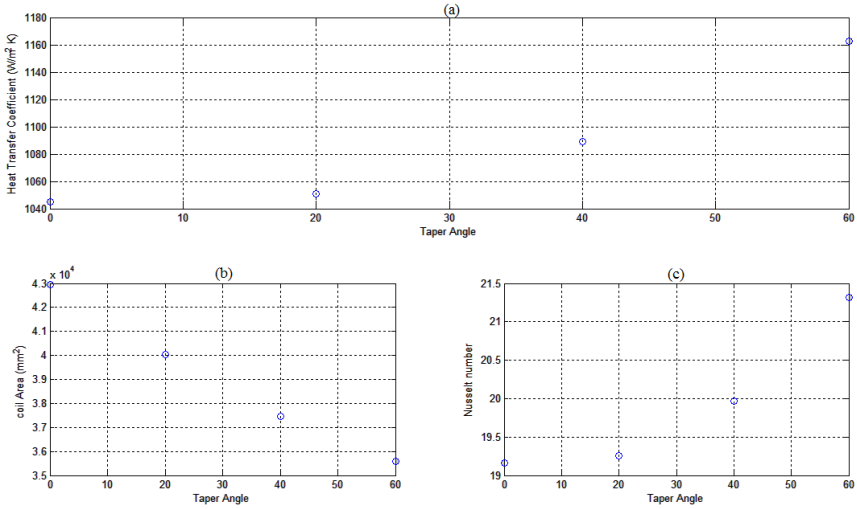

Fig. 16. The Effect of the Taper angle on the Area, Heat Transfer Coefficient and Nusselt Number (R = 75, a=12.5).

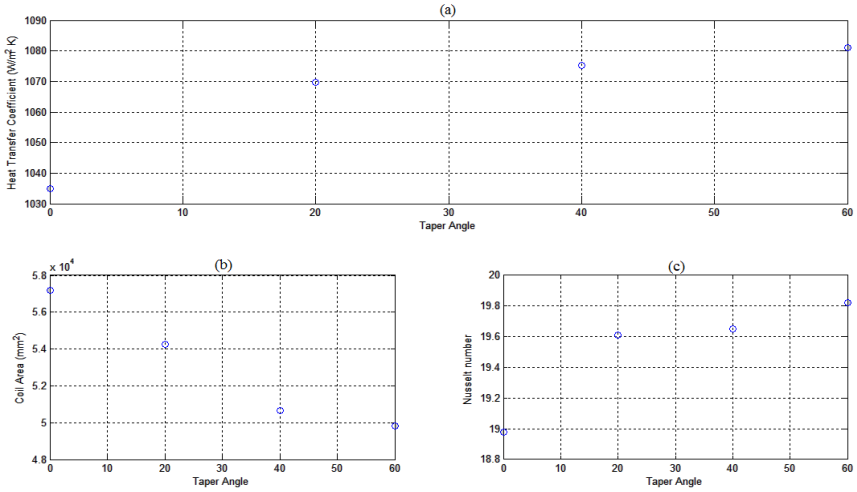

Fig. 17. The Effect of the Taper Angle on the Area, Heat Transfer Coefficient and Nusselt Number (R = 100, a = 12.5).

4. Conclusions

In the first and second scenario the heat transfer coefficient and Nusselt number were found to increase when increasing the taper angle of the helical cone coil, and that was attributed to the increase in the curvature ratio and thus Dean Number which is accompanied by the increase in the taper angle.

The coil exit temperature in the first scenario tended to increase with the taper angle and that was attributed to the increase in both coil area and the Dean number (which increases with increasing the taper angle, leading to an increase in the heat transfer coefficient), while in the second scenario the coil exit temperature tended to decrease in spite of the increase in the heat transfer coefficient and that was

attributed to the significant reduction in the coil area as in that case both the height and the pitch were multiplied by cosine the taper angle. The helical cone coil would require less space for installation (both in the first and second scenarios) but the increase in the taper angle increased the area of heat transfer (first scenario) leading to better heat transfer than that of the ordinary helical coil.

To transform an existing ordinary helical coil to a helical cone coil and benefit from the enhanced heat transfer characteristics and the lower space requirement; the first scenario is recommended to be adopted.

References

1. Rohsenow, W.M.; Hartnett, J.R.; and Cho, Y.I. (1998). *Handbook of heat transfer*. (3rd Ed.), McGraw-Hill Professional, New York.
2. Dean, W.R. (1927). Note on the motion of fluid in a curved pipe. *Philosophical Magazine, Series* 7, 4(20), 208-233.
3. Dean, W.R. (1928). The stream line motion of fluid in a curved pipe, *Philosophical Magazine, Series* 7, 5(30), 673–695.
4. Eustice, J. (1911). Experiments on stream-line motion in curved pipes. *Proceedings of the Royal Society of London*, *Series A*, *Mathematical and Physical Sciences*, 85(576), 119-131.
5. White, C.M. (1929). Streamline flow through curved pipes. *Proceedings of the Royal Society of London*, *Series A*, *Mathematical and Physical Sciences*, 123(792), 645-663.
6. Hawthorne, W.R. (1951). Secondary circulation in fluid flow. *Proceedings of the Royal Society of London*, *Series A*, *Mathematical and Physical Sciences*, 206(1086), 374-387.
7. Horlock, J.H. (1956). Some experiments on the secondary flow in pipe bends. *Proceedings of the Royal Society of London, Series A, Mathematical and Physical Sciences*, 234(1198), 335-346.
8. Barua, S.N. (1963). On secondary flow in stationary curved pipes. *The Quarterly Journal of Mechanics and Applied Mathematics*, 16(1), 61-77.
9. Austin, L.R.; and Seader, J.D. (1973). Fully developed viscous flow in coiled circular pipes. *AIChE Journal*, 19(1), 85-94.
10. Behjan, A.; and Kraus, A.D. (2003). *Heat transfer handbook*. Wiley-Interscience.
11. Srinivasan, P.S.; Nandapurkar, S.S.; and Holland, F.A. (1968). Pressure drop and heat transfer in coils. *The Chemical Engineer*, 218, 113-119.
12. Dennis, S.C.R. and Ng, M. (1982). Dual solutions for steady laminar flow through a curved tube. *The Quarterly Journal of Mechanics and Applied Mathematics*, 35(3), 305-324.
13. Dennis, S.C.R. and Riley, N. (1991). On the fully developed flow in a curved pipe at large Dean number. *Proceedings of the Royal Society of London*, *Series A*, *Mathematical and Physical Sciences*, 434(1891), 473-478.
14. Austen, D.S., and Soliman, H.M. (1988). Laminar flow and heat transfer in helically coiled tubes with substantial pitch. *Experimental Thermal and Fluid Science*, 1(2), 183-194.

15. Yang, G.; Dong, Z.F.; and Ebadian, M.A. (1995). Laminar forced convection in a helicoidal pipe with finite pitch. *International Journal of Heat and Mass Transfer*, 38(5), 853-862.
16. Germano, M. (1982). On the effect of torsion on a helical pipe flow. *Journal of Fluid Mechanics*, 125, 1-8.
17. Tuttle, E.R. (1990). Laminar flow in twisted pipes. *Journal of Fluid Mechanics*, 219, 545-570.
18. Kalb, C.E.; and Seader, J.D. (1972). Heat and mass transfer phenomena for viscous flow in curved circular tubes. *International Journal of Heat and Mass Transfer*, 15(4), 801-817.
19. Zapryanov, Z.; Christov, Ch.; and Toshev, E. (1980). Fully developed laminar flow and heat transfer in curved tubes. *International Journal of Heat and Mass Transfer*, 23(6), 873-880.
20. Futagami, K.; and Yoshiyuki, A. (1988). Laminar heat transfer in a helically coiled tube. *International Journal of Heat and Mass Transfer*, 31(2), 387-396.
21. Figueiredo, A.R., and Raimundo, A.M. (1996). Analysis of the performances of heat exchangers used in hot-water stores. *Applied Thermal Engineering*, 16(7), 605-611.
22. Naphon, P.; Suwagrai, J. (2007). Effect of curvature ratios on the heat transfer and flow developments in the horizontal spirally coiled tubes, *International Journal of Heat and Mass Transfer*, 50(3-4), 444-451.
23. Ke, Y.; Pei-qi, G.; Yan-cai, S.; and Hai-tao, M. (2011). Numerical simulation on heat transfer characteristic of conical spiral tube bundle. *Applied Thermal Engineering*, 31(2-3), 284-292.
24. Manlapaz, R.L.; and Churchill, S.W. (1980). Fully developed laminar flow in a helically coiled tube of finite pitch. *Chemical Engineering Communications*, 7(1-3), 57-78.